

# Line-of-Sight Angle of Arrival Estimation in the Outdoor Multipath Environment

Richard Klukas and Michel Fattouche

**Abstract**— Angle of arrival (AOA) estimation utilizing the Multiple Signal Identification and Classification (MUSIC) algorithm is investigated for land vehicle location systems. A “virtual” antenna array is used to overcome problems inherent to MUSIC when operating in a highly correlated signal environment. Based on assumptions regarding the multipath radio environment, triangulation is possible by estimating the AOA of the line-of-sight (LOS) component in the received signal. Computer simulations are used to analyze the ability of techniques incorporating MUSIC to achieve this. Since triangulation is achieved in this paper using a narrowband signal, no new spectrum is required. Instead, the current cellular telephone bands as well as the existing base-station hardware could be exploited resulting in a cost-efficient and easily implemented system. A further cost reduction may be realized by processing received signal data while travelling along a nonlinear trajectory. In this way, an unambiguous angular spectrum is obtained with one antenna.

**Index Terms**—Angle of arrival, AOA, AOA estimation, cellular, cellular telephone positioning, multipath, MUSIC, superresolution, triangulation.

## I. INTRODUCTION

**R**ADIO triangulation is a method of estimating position by finding the angle of arrival (AOA) of radio waves transmitted from two or more sources. Obviously, the success of triangulation hinges on the existence of a direct propagation path between each of the transmitters and the receiver. For this reason, triangulation has traditionally not been used for land vehicle location systems because of the multipath nature of the radio propagation environment in urban areas. Reflections of radio signals by obstacles such as large buildings or rugged topography can cause large positional errors even when a direct path exists between each of the transmitters and the receiver. The accuracy of the position fix of course depends on the accuracy of the AOA estimate. As the distance between the transmitters and receiver increases, so does the error in absolute location for a given error in the AOA estimate. A system to estimate AOA in multipath environments using multibeam antennas and thereby estimate vehicle positions has been presented in the literature [1]. The authors report rms position errors of 200–300 m. This paper presents an alternate method of estimating AOA, which achieves an rms position error of 100 m or less.

Manuscript received June 15, 1993; revised March 29, 1995 and May 9, 1996. This work was supported by the National Science and Engineering Research Council of Canada (NSERC), TRILabs, and the University of Calgary.

R. Klukas is with Cell-Loc, Inc., Calgary, Alberta, T2E 7N6, Canada (e-mail: rklukas@ensu.ucalgary.ca).

M. Fattouche is with the University of Calgary, Cell-Loc, Inc. and TRILabs, Calgary, Alberta, T2L 2K7, Canada (e-mail: michel@cell-loc.com).

Publisher Item Identifier S 0018-9545(98)00103-0.

Although much of the arrival direction distribution of radio waves in the multipath environment is still unknown, recent research [2] indicates that radio waves originating from a single source are scattered and reflected in such a way that they tend to arrive at a distant point in clusters. It is assumed that the first cluster to arrive has the larger magnitude and is attributed to the direct ray as well as reflections near the antenna. The other clusters are composed of reflected rays which travel longer and more attenuated paths.

The outdoor multipath radio environment is also assumed to exhibit this clustering effect [3]. If a line-of-sight (LOS) cluster exists, its arrival angle is the information required to locate a vehicle by triangulation. It is assumed that the distance between transmitter and receiver is sufficiently large that AOA may be measured in the horizontal plane. Therefore, throughout this paper AOA refers to azimuth not elevation.

Numerous methods to estimate AOA exist. Parametric methods, which employ eigenanalysis of the data correlation matrix, provide very accurate estimates of arrival angle and far higher resolution compared to other methods such as the Fourier transform [4]. One such parametric method, the Multiple Signal Identification and Classification (MUSIC) algorithm, is briefly described in Section II. In particular, the application of MUSIC to the mobile, multipath environment is described. Section III presents the results of the computer simulations conducted. First addressed is the ability of MUSIC to estimate the AOA of individual arrivals as well as that of a cluster of arrivals. Three techniques are then presented which identify the LOS cluster in the presence of two other clusters. Following the identification of the LOS cluster and an estimation of its AOA, a fourth technique is used to estimate the AOA of the LOS component within the cluster. Section IV concludes the paper by demonstrating how an unambiguous spatial spectrum may be obtained with a single antenna following a nonlinear trajectory.

## II. THE MUSIC ALGORITHM

The MUSIC algorithm is an eigenanalysis direction finding method, which has demonstrated superior performance in terms of accuracy and resolution over other parametric methods such as maximum likelihood and maximum entropy [5], [6]. It requires a multielement antenna array in order to form a correlation matrix using data received by the array. Eigendecomposition of the correlation matrix results in two sets of eigenvalues.

- 1) A first set which corresponds to the  $M-K$  smallest eigenvalues.

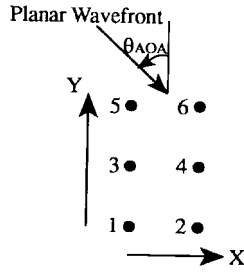


Fig. 1. Two-dimensional antenna array.

- 2) A second set which corresponds to the  $K$  largest eigenvalues;  $K$  being the number of narrowband signals impinging on an  $M$  element array.

The requirement of the multielement array is the first obstacle to be overcome when applying MUSIC to the problem of estimating AOA at a land vehicle. A multielement antenna array mounted on an automobile is impractical, costly, and not aesthetically pleasing. An alternative to a physical array is to use a fewer number of physical antennas and exploit the motion of the vehicle. A “virtual” array is produced by sampling in time, one or more vehicle mounted antennas as the vehicle moves. This results in spatially and temporally separated samples which mimic an antenna array. If the distance over which sampling occurs is relatively small, the signal environment will not change significantly from the time of the first sample to the time of the last.

MUSIC does not restrict the geometry of the array but merely requires knowledge of it. This knowledge is contained in the steering vector. Consider the virtual array for two physical antennas, shown in Fig. 1. The direction of motion is in the direction  $Y$  and the AOA is measured as shown. Due to the cosine and sine functions used in calculating the steering vector, an ambiguity exists if the array is one dimensional (1-D). If the array of Fig. 1 consists of only elements 1, 3, and 5, the MUSIC spectrum from  $0^\circ$  to  $180^\circ$  will be identical to that of  $360^\circ$  back to  $180^\circ$ . However, if a two-dimensional (2-D) array is used, the angular spectrum will be unique throughout the entire  $360^\circ$ . Therefore, if the vehicle travels in a straight line, at least two physical antennas mounted such that the line connecting them is perpendicular to the direction of motion, are required. Section IV shows that when the vehicle travels a nonlinear trajectory, such an ambiguity can be removed using only one physical antenna.

Eigenanalysis methods such as MUSIC breakdown when two or more of the arriving signals are highly correlated. In a multipath environment, the signals are almost always correlated to some extent. Effective decorrelation of the signals is necessary to ensure proper operation of MUSIC. Vehicle motion in itself will decorrelate the signals due to the existence of Doppler shifts in a mobile environment. This assumes that the signals have unique arrival angles and the time averaging operation inherent in obtaining the correlation matrix covers many differential Doppler cycles [6].

A second method of decorrelating signals is spatial smoothing. If an antenna array consists of  $M$  elements, a subarray is formed consisting of  $N$  elements, where  $N < M$ . Spatial smoothing is then introduced by sliding the subarray across

the full array in both the forward and backward directions. Interested readers may refer to [7] for details concerning spatial smoothing.

Whereas spatially spread data collected by an array is required to solve for AOA, estimating the frequencies of sinusoids impinging on a single antenna requires a time series of data. The two algorithms are similar except that the steering vector in the spatial case is replaced by a frequency scanning vector in the temporal [4]. For those frequencies which correspond to the angular frequencies of the sinusoids contained in the data, the frequency scanning vector will be orthogonal to the noise subspace spanned by the eigenvectors corresponding to the  $M-K$  smallest eigenvalues. The AOA  $\theta_{\text{AOA}}$  of the sinusoid corresponding to a Doppler shift  $\omega$  may be determined from the relation

$$2\pi \frac{V}{\lambda} \cos(\theta_{\text{AOA}}) = \omega$$

where  $V$  is the velocity of the vehicle and  $\lambda$  is the wavelength of the transmitted signal. The cosine function in the above equation again results in an ambiguity. As in the case of spatial MUSIC, two physical antennas will resolve the ambiguity. Once the frequency of a signal is known, its amplitude and phase may also be determined. The phase of a signal at each of the two antennas may then be used to resolve the ambiguity.

A final restriction on MUSIC to ensure its success is for the collected data to be of narrowband nature. This can be readily achieved in the current North American cellular system using the existing supervisory audio tone (SAT) tone. Thus, no new spectrum is required. This is the main advantage of this system compared to spread-spectrum systems [8].

### III. COMPUTER SIMULATIONS

#### A. Simulation Data

Simulation data was provided by SURP, a simulation program for the urban multipath propagation channel [9]. SURP models the clustering of paths as suggested by Turin [10] and developed by Suzuki [11]. The arrival times are modeled by a modified Poisson process or  $\Delta$ - $K$  model. The  $K'$  values for the 76 bin discrete time  $\Delta$ - $K$  model are given in Table I.

The signal amplitudes are simulated with a lognormal distribution. For paths close to LOS, signal strength follows the Nakagami distribution while other paths follow the lognormal distribution. Due to the complexity of the simulation program however, the lognormal distribution was used for all signal amplitudes. The path strengths are both spatially and temporally correlated. For the simulations performed, the temporal correlation coefficients for initial, adjacent paths are typically between 0.4–0.6. For example, between paths 1 and 2, the correlation coefficient was 0.56 and between paths 2 and 3, 0.488. Spatial correlation between components is determined by AOA as will be discussed later. Carrier frequencies of 800 and 840 MHz were chosen since they lie in the applicable cellular spectrum. The amplitude and time delays, however, were simulated for SURP's channel 2 at 1280 MHz.

SURP simulates data for four different environments. For the purpose of this work, area B, which represents the downtown part of a medium-size city such as Oakland, was chosen.

TABLE I  
 $K'$  VALUES FOR DISCRETE TIME  $\Delta$ - $K$  MODEL

0.494	0.494	0.494	0.494	0.494	0.494	0.494	0.494
0.494	0.494	0.402	0.385	0.368	0.351	0.334	0.542
0.553	0.564	0.575	0.586	0.480	0.480	0.480	0.480
0.480	1.354	1.421	1.488	1.555	1.622	0.648	0.648
0.648	0.648	0.648	0.648	0.648	0.648	0.648	0.648
0.648	0.648	0.648	0.648	0.648	0.648	0.648	0.648
0.648	0.648	0.648	0.648	0.648	0.648	0.648	0.648
0.648	0.648	0.648	0.648	0.648	0.648	0.648	0.648
0.648	0.648	0.648	0.648	0.648	0.648	0.648	0.648
0.648	0.648	0.648	0.648	0.648	0.648	0.648	0.648
0.648	0.648	0.648	0.648				

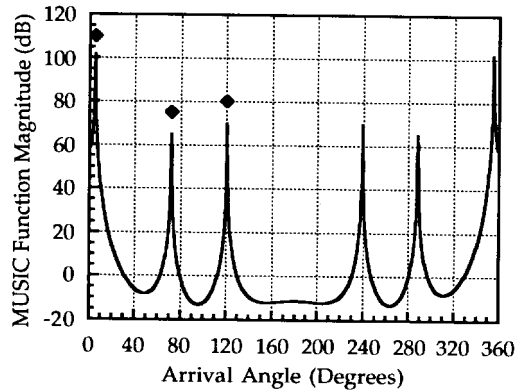


Fig. 2. Results for a one antenna by six virtual element array.

This area was chosen on the advise of Hashemi who displays the most confidence in area B data [12]. It is also the second most extreme environment in terms of multipath and therefore a reasonable choice for a typical environment.

### B. Resolving Individual Arrivals

Fig. 2 illustrates the spatial MUSIC spectrum for a single antenna moving in a straight line at 100 km/h. The antenna's received signal is sampled at six equally spaced points, which cover a total distance of 62 cm ( $0.33\lambda$  between points at 800 MHz). The simulated signal environment consists of three distinct arrivals all originating from a transmitted tone of frequency 800 MHz. The AOA of the three arrivals are indicated by the black diamonds in the figure. Fig. 2 clearly indicates that MUSIC is able to detect the three arrivals and estimate their AOA very accurately. For a spectrum resolution of one-half degree, the accuracy is within two tenths of a degree. However, the ambiguity problem is clearly evident. The spectrum is folded around  $180^\circ$ . Fig. 3 shows that a 2-D array created by sampling two antennas at three equally spaced points overcomes this problem. The two antennas are separated by  $0.5\lambda$  (18.75 cm) and the total distance from the first sampled point to the third is 28 cm ( $0.37\lambda$  between points at 800 MHz).

### C. Resolving a Cluster AOA

In a multipath environment, resolving for all of the individual arrivals is not necessarily desired. Instead, the average AOA of the cluster as a whole may be all that is required.

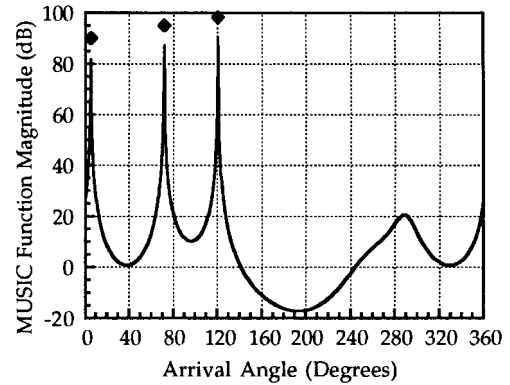


Fig. 3. Results for a two antenna by three virtual element array.

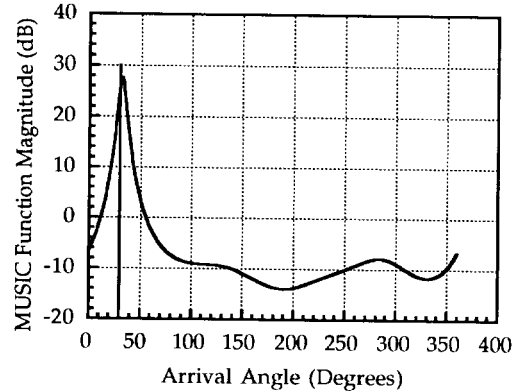


Fig. 4. Resolving the base-station angle in the presence of multipath.

Fig. 4 illustrates the MUSIC spectrum for one such case. The signal environment is simulated as a cluster of 13 arrivals spread around  $30^\circ$  by  $\pm 25^\circ$ . All 13 arrivals originate from a single 800 MHz transmission. A  $2 \times 2$  virtual antenna array is used. The physical antennas are again separated by  $0.5\lambda$  and the distance between the two sampled points is 12 cm. The vehicle velocity is 100 km/h. The spectrum in Fig. 4 is generated by allocating only the eigenvalue of largest magnitude to the signal subspace. The mean AOA of the 13 simulated arrivals is  $30^\circ$ , which is the desired AOA to be estimated by MUSIC. The MUSIC peak in Fig. 4 is only  $2^\circ$  in error with respect to the vertical line at  $30^\circ$ .

To determine the effect of cluster width, the same simulation as above is carried out with varying cluster widths. The result is shown in Fig. 5, where the solid line corresponds to the

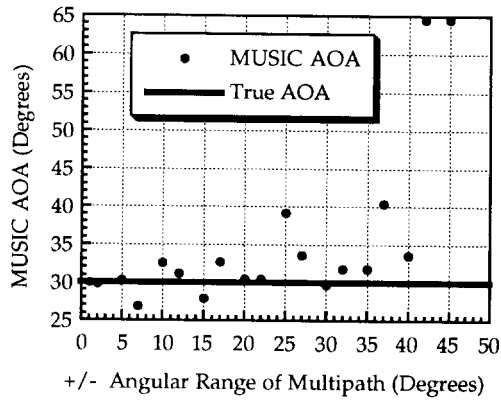


Fig. 5. Performance of MUSIC with increasing multipath.

true AOA and the dots correspond to the MUSIC estimate for specific cluster widths. Until the cluster reaches a width of approximately  $80^\circ$  ( $\pm 40^\circ$ ), the error in the cluster AOA is in all but two cases less than  $5^\circ$ . It is important to note that the clusters used are symmetrical. That is the angle of the transmitter with respect to the receiving array is assumed to be the center of the cluster.

#### D. The Three-Cluster Environment

The signal environment assumed for the channel between any one transmitter and a vehicle is illustrated in Fig. 6. Three clusters are assumed here. The first cluster of signals to arrive corresponds to the LOS path. It contains 13 arrivals, which have a mean power of  $-15.9$  dBW. The second and third clusters to arrive contain six and four arrivals with mean powers of  $-18.2$  dBW and  $-20.5$  dBW, respectively. This is somewhat comparable to the IS-54 cellular standard [3], which models the mobile cellular radio channel as two independently fading Rayleigh channels. However, it should be emphasized that the signal amplitudes simulated by SURP follow the lognormal distribution.

#### E. Technique #1—Petra

The PEAK TRacking Algorithm (PETRA) was developed to determine the LOS cluster in a three-cluster environment by tracking the dominant peak in the MUSIC spectrum as the number of allocated signal subspace eigenvalues varies from one to three. PETRA is based on the assumption that when the signal space is defined by only one eigenvector, the dominant peak in the MUSIC spectrum will correspond to that signal (or cluster) with the highest power. If the LOS cluster is of the highest power, then the dominant MUSIC peak should estimate its AOA.

PETRA employs spatial MUSIC with temporal smoothing. Temporal smoothing is a method of forming the data correlation matrix from snapshots of data, which are temporally spaced [4]. Since the antennas are sampled while moving, temporal smoothing is essentially the same as spatial smoothing.

The process of tracking the dominant peak for one, two, and three signal eigenvalues is as follows.

- 1) Find the eigenvalues and corresponding eigenvectors of the data correlation matrix.

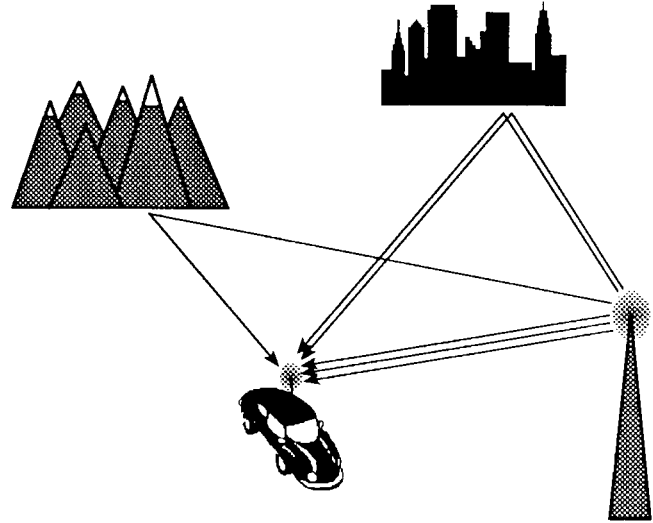


Fig. 6. Signal-cluster environment.

- 2) Define the signal subspace as that space spanned by the eigenvector corresponding to the eigenvalue of highest magnitude; the remaining eigenvectors span the noise subspace.
- 3) Generate the MUSIC spectrum for the partition specified in 2) and note the AOA of the dominant peak.
- 4) Repartition the eigenvalues and eigenvectors found in 1) such that the two highest magnitude eigenvalues are attributed to signals and the remaining to noise.
- 5) Generate another MUSIC spectrum based on the partition in 4) and note the AOA of the peak closest to the AOA found in 3).
- 6) Repeat step 4) with three signal eigenvalues.
- 7) Generate another MUSIC spectrum based on the partition in 6).
- 8) The AOA of the peak closest to the AOA determined in 5) will be the estimate of the AOA of the LOS cluster.

The AOA of the LOS, second, and third clusters are chosen to be  $240^\circ$ ,  $300^\circ$ , and  $90^\circ$ , respectively. A  $2 \times 2$  array, with 50 data samples per element and a virtual element spacing of 14 cm is used. The two physical antennas are separated by  $0.5\lambda$  (18 cm). The speed of the mobile is 50 km/h.

The angular width of the clusters is varied from  $2^\circ$  to  $80^\circ$  (all three clusters always having the same width) and PETRA is run on ten consecutive sets of data for each cluster width. Thus, there are ten trials for each cluster width. For each trial, the dominant MUSIC peak for one signal eigenvalue and the corresponding peaks for two and three signal eigenvalues are recorded. The results for the dominant peak for one signal eigenvalue are shown in Fig. 7. The bold horizontal line in Fig. 7 corresponds to the true AOA of the LOS cluster at  $240^\circ$ , whereas the dots correspond to the dominant MUSIC peaks for the ten trials at each cluster width. Clearly illustrated is the fact that the majority of dominant peaks correspond to the LOS cluster at  $240^\circ$ . Dots in the vicinity of  $300^\circ$  and  $90^\circ$  demonstrate that occasionally the other clusters will dominate.

Fig. 8 shows the results for two- and three-signal eigenvalues. The average of the ten trials at each cluster width has been shown instead of the individual results. Recall that for

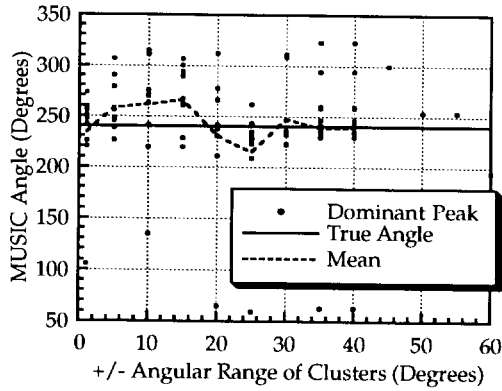


Fig. 7. Dominant peak angle for one-signal eigenvalue.

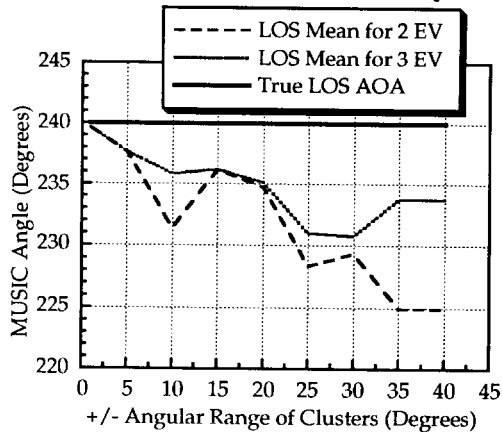


Fig. 8. Mean comparisons for two- and three-signal eigenvalues.

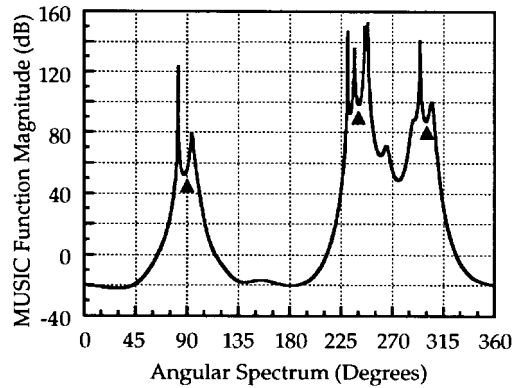


Fig. 9. Resolving multiple arrivals with technique #2.

one-signal eigenvalue, the AOA of the dominant peak is of interest. For two- and three-signal eigenvalues however, the peak closest in AOA to the estimate made with one- and two-signal eigenvalues, respectively, is the LOS estimate. Fig. 8 clearly demonstrates two points. First, the LOS AOA estimate becomes more accurate as the number of signal eigenvalues increases; second, as the width of the clusters increases, the LOS estimates tend to drift away from the true value of  $240^\circ$ .

The results of Figs. 7 and 8 illustrate that PETRA must be run over several data sets in order to be reliable and accurate. Since the LOS cluster is not always properly identified, enough PETRA estimates must be generated to obtain a clear LOS majority. It was also determined that the accuracy of the

individual PETRA estimates is very poor. If, however, many LOS PETRA estimates are averaged, the resulting error is much smaller.

To obtain a more statistical appreciation for the performance of PETRA, simulations were run for 15 different sets of clusters. The cluster angles were randomly selected and the angular width of all clusters was  $50^\circ (\pm 25^\circ)$ . For each cluster set, PETRA estimated the AOA of the LOS cluster for 200 consecutive data sets. Again, a  $2 \times 2$  virtual antenna array was used. The spacing between the physical antennas and between the virtual antennas was 18 cm, which is  $0.5\lambda$  at a frequency of 840 MHz (all of the following simulations were performed at 840 MHz). For a sampling interval of  $41.6 \mu\text{s}$  and a speed of 50 km/h, virtual elements were separated by 309 data points. This required a total of 123 600 data points, which cover a distance of  $200\lambda$  or 71.4 m at the given frequency. At 50 km/h, this distance is travelled in 5.1 s. The results of these simulations are given in Table II. The cluster angles listed in the second column for each particular set, are listed in the order of arrival. Hence, the first angle is the true LOS cluster AOA.

The statistics presented in Table II are specific to those AOA estimates made by PETRA, which correspond to the true LOS AOA. Take set 1 as an example. Of the 200 AOA estimates made, 161 of them identified the LOS cluster as opposed to one of the other two clusters. The mean value of the 161 AOA estimates was  $236.6^\circ$ , which is  $3.4^\circ$  in error with respect to the true LOS cluster angle of  $240^\circ$ . The variance of the 161 estimates is  $170.1^\circ$ .

Overall, PETRA correctly identified the LOS cluster 66% of the time, and the mean LOS error was  $5.7^\circ$ . This confirms that a large number of estimates must be averaged in order to obtain an accurate AOA estimate. The AOA error may be reduced if a more sophisticated method of grouping the estimates was used. The method used to generate the results of Table II was a simple boundary technique, where estimates, which clearly do not belong to any cluster, are included in the closest cluster group.

Although a reasonable degree of accuracy is obtained with PETRA, the need for many estimates in order to obtain a LOS majority and an accurate AOA estimate is a serious drawback. The following two techniques attempt to overcome this problem while maintaining the same degree of accuracy.

#### F. Technique #2—Resolving Many Arrivals

A second method of determining the AOA of the LOS cluster is to resolve for as many of the individual arrivals as possible. If it is true that the LOS cluster contains more arrivals than any other cluster, that group of arrivals in the angular spectrum, which contains the largest number of arrivals will correspond to the LOS cluster.

Fig. 9 demonstrates how the LOS cluster is recognizable by the number of arrivals. This spectrum was obtained by moving two physical antennas separated by  $0.5\lambda$  (18 cm) at a speed of 50 km/h and sampling 18 times over a distance of 1.8 m. Forward and backward spatial smoothing was used to provide more decorrelation between the arriving signals. The three clusters are each  $20^\circ (\pm 10^\circ)$  wide, and their centers are indicated by the black pointers. The LOS cluster is at  $240^\circ$ ,

TABLE II  
PETRA SIMULATION RESULTS

Set	Cluster Angles	No. of LOS Solutions	Mean of LOS Solutions	Variance of LOS Solutions	Abs., Mean LOS Err.
1	240° 300° 90°	161/200	236.6°	170.1° <sup>2</sup>	3.4°
2	120° 40° 200°	130/200	122.8°	286.9° <sup>2</sup>	2.8°
3	325° 175° 115°	151/200	323.4°	361.1° <sup>2</sup>	1.6°
4	180° 240° 270°	129/200	174.2°	659.8° <sup>2</sup>	5.8°
5	328° 271° 295°	108/200	345.2°	1920.5° <sup>2</sup>	17.2°
6	19° 174° 321°	169/200	19.0°	164.8° <sup>2</sup>	0.02°
7	250° 275° 79°	124/200	238.0°	276.3° <sup>2</sup>	12.0°
8	226° 84° 137°	159/200	239.4°	480.8° <sup>2</sup>	13.4°
9	331° 67° 243°	108/200	329.7°	115.2° <sup>2</sup>	1.4°
10	319° 300° 45°	90/200	326.7°	131.2° <sup>2</sup>	7.7°
11	86° 352° 158°	100/200	91.9°	152.9° <sup>2</sup>	5.9°
12	206° 322° 138°	119/200	193.0°	189.1° <sup>2</sup>	12.9°
13	180° 235° 0°	146/200	180.2°	72.0° <sup>2</sup>	0.2°
14	59° 339° 320°	112/200	58.8°	322.9° <sup>2</sup>	0.2°
15	216° 7° 278°	153/200	215.5°	323.0° <sup>2</sup>	0.5°
<b>Average</b>	-	<b>131/200</b>	-	<b>375.1°<sup>2</sup></b>	<b>5.7°</b>

TABLE III  
SIMULATION RESULTS FOR TECHNIQUE #2

Set	Cluster Angles	No. of LOS Solutions	Percent by Peak Count	Percent by Peak Magnitude	RMS LOS Error with respect to:	
					centre	average
1	240° 300° 90°	19/20	84.2%	15.8%	4.5°	5.0°
2	120° 40° 200°	16/20	81.3%	18.7%	2.9°	3.0°
3	325° 175° 115°	17/20	76.5%	23.5%	4.1°	5.4°
4	180° 240° 270°	0/20	-	-	-	-
5	328° 271° 295°	3/20	66.7%	33.3%	1.9°	4.0°
6	19° 174° 321°	11/20	63.6%	36.4%	5.2°	6.2°
7	250° 275° 79°	5/20	20%	80%	5.2°	4.1°
8	226° 84° 137°	16/20	93.8%	6.2%	19.5°	11.4°
9	331° 67° 243°	7/20	57.1%	42.9%	2.8°	3.9°
10	319° 300° 45°	20/20	100%	0%	13.2°	13.8°
11	86° 352° 158°	19/20	94.7%	5.3%	3.6°	2.9°
12	206° 322° 138°	1/20	100%	0%	0.5°	7.3°
13	180° 235° 0°	0/20	-	-	-	-
14	59° 339° 320°	18/20	61.1%	38.9%	5.0°	5.9°
15	216° 7° 278°	20/20	80%	20%	4.1°	3.6°
<b>Mean</b>	-	<b>11.5/20</b>	<b>75.3%</b>	<b>24.7%</b>	<b>5.6°</b>	<b>5.9°</b>

the second cluster at 300°, and the third at 90°. Although all 23 arrivals of the three clusters are not resolved, there are obviously more arrivals grouped around 240° than anywhere else.

Simulations were repeated on the same 15 cluster sets tested with technique #1. Again, two physical antennas separated by  $0.5\lambda$  (18 cm) were used. The number of virtual elements per physical antenna was 24, resulting in a  $2 \times 24$  array. The virtual elements were separated by  $0.32\lambda$ . For a speed of 50 km/h and a sampling interval of  $41.6 \mu\text{s}$ , a total of 92 480 data points were separated into 20 data sets. At 50 km/h, the distance travelled for the 20 data sets is 53.4 m. Spatial MUSIC with

forward and backward spatial smoothing was asked to resolve for ten signals. The results for these simulations are shown in Table III.

The “No. of LOS solutions” refers to the number of simulations out of 20 in which the cluster chosen as LOS was indeed the true LOS cluster. This number is further broken down in the next two columns of Table III. In the event that two clusters had an equal number of arrivals, the magnitude of the MUSIC peaks were used to make the decision. In such a case, the cluster with the highest average magnitude of peaks was chosen as LOS. Hence, “percent by peak count” refers to the percentage of LOS solutions which were chosen because that

TABLE IV  
SIMULATION RESULTS FOR TECHNIQUE #3

Set	Cluster Angles	% of Valid Solutions	RMS Valid Error w.r.t.		% of LOS Solutions	RMS LOS Error with respect to:	
			centre	average		centre	average
1	240° 300° 90°	66%	11.1°	11.0°	66%	11.1°	11.0°
2	120° 40° 200°	38%	32.7°	28.8°	30%	11.1°	8.5°
3	325° 175° 115°	42%	66.6°	67.2°	34%	11.0°	11.2°
4	180° 240° 270°	58%	32.0°	32.0°	40%	19.2°	19.2°
5	328° 271° 295°	58%	25.8°	27.5°	38%	12.6°	13.9°
6	19° 174° 321°	64%	30.3°	31.8°	42%	12.9°	8.4°
7	250° 275° 79°	54%	15.8°	14.3°	54%	15.8°	14.3°
8	226° 84° 137°	70%	29.8°	33.6°	64%	10.3°	14.7°
9	331° 67° 243°	52%	11.8°	11.8°	52%	11.8°	11.8°
10	319° 300° 45°	54%	27.1°	27.0°	44%	9.8°	9.7°
11	86° 352° 158°	16%	30.1°	30.6°	10%	8.4°	7.6°
12	206° 322° 138°	48%	36.7°	36.4°	34%	8.8°	13.9°
13	180° 235° 0°	58%	31.0°	31.0°	28%	18.6°	18.6°
14	59° 339° 320°	56%	38.4°	38.0°	46%	14.5°	14.4°
15	216° 7° 278°	58%	32.3°	31.2°	52%	9.0°	7.7°
<b>Mean</b>	<b>-</b>	<b>52.8%</b>	<b>30.1°</b>	<b>30.1°</b>	<b>42.3%</b>	<b>12.3°</b>	<b>12.3°</b>

cluster contained the most peaks. “Percent by peak magnitude” corresponds to the cases in which there was a tie and the cluster with the highest average peak magnitude was chosen. Take set 1 as an example. In 19 out of the 20 simulations, the cluster chosen as LOS was indeed the LOS cluster. In 16 out of those 19 simulations (84.2%), the cluster was chosen because it contained the most arrivals. In the other three of the 19 simulations (15.8%), there was a tie and the correct cluster was chosen because of peak magnitude.

The average AOA of the peaks in the group with the highest number of arrivals, was taken as the estimate of the LOS cluster AOA. The rms error in the AOA estimates was calculated with respect to the spatial center of the Hashemi LOS cluster as well as the average AOA of that cluster. The results indicate that there is little if any bias in the Hashemi LOS clusters.

Although the rms error in the LOS estimates is less than 6°, two serious difficulties were encountered. First, in many cases, the peaks in the MUSIC spectrum were not clearly segregated as in Fig. 9. As a result, it was difficult to cluster the arrivals in an entirely objective manner. This in part led to the second problem. For six of the 15 cluster sets tested, the most numerous group of arrivals did not correspond to the actual LOS cluster for the majority of the 20 data sets. This usually occurred when clusters were very close in terms of AOA. Either the LOS cluster was close to one of the other clusters making the clustering of arrivals difficult, or the second and third clusters were so close that they were impossible to distinguish and hence formed the largest group.

#### G. Technique #3—Temporal Music

A third technique to estimate the AOA of the LOS cluster utilizes temporal MUSIC and signal amplitude information. Whereas technique #2 uses the number of arrivals as the criteria to determine which cluster is LOS, technique #3

depends on the assumption that the LOS cluster contains the most power. The technique is simple. Resolve for three arrival Doppler frequencies and use these frequencies to determine the corresponding arrival amplitudes. Choose the arrival with the largest amplitude and convert the Doppler frequency to AOA.

Simulations for the same 15 cluster sets tested with techniques #1 and #2 were performed for two physical antennas separated by  $0.25\lambda$  (9 cm). Since only three arrivals are resolved, fewer points are required than for technique #2. Fifty data sets of 5 points (virtual elements) each were used. The points were spaced by  $0.07\lambda$ . At 50 km/h, five points are collected in 9.5 cm. This is also far fewer points than was necessary with PETRA, since forward and backward smoothing were used in technique #3.

The simulation results are presented in Table IV. The “% of valid solutions” is the number of simulations, as a percentage of 50, which are valid in the sense that the angular ambiguity of the resolved signal of highest amplitude could be eliminated. The “rms valid error” is the rms error of the valid solutions calculated with respect to the spatial center of the Hashemi LOS cluster and with respect to the average arrival angle of the Hashemi LOS cluster. The next three columns contain the same type of information, but only for the LOS solutions within the valid solutions. LOS solutions are those for which the absolute error is less than 25°. Any solution with an error greater than 25° is considered to correspond to a non-LOS cluster. The “% of LOS solutions” is also represented as a percentage of 50.

Based on the amplitude of the resolved arrivals, the actual LOS cluster was, on the average, properly identified only 52.8% of the time. In general, incorrect solutions were not due to the true LOS arrival having a lower amplitude than the others. Instead, errors in the phase at each of the two antennas made elimination of the cosine ambiguity impossible. This may be due to the degree of nonsingularity of the matrix,

TABLE V  
SIMULATION RESULTS FOR ONE-CLUSTER TESTS

Cluster	Cluster AOA	LOS AOA	% of Valid Solutions	RMS Error
1	240°	237.1°	70%	5.2°
2	120°	120.6°	85%	1.3°
3	325°	325.5°	75%	2.5°
4	180°	177.5°	60%	13.5°
5	328°	328.7°	80%	3.3°
6	19°	18.6°	90%	2.1°
7	250°	247.3°	75%	2.3°
8	226°	221.5°	80%	3.2°
9	331°	330.6°	90%	2.3°
10	319°	318.0°	80%	4.3°
11	86°	79.8°	75%	0.9°
12	206°	207.0°	100%	2.5°
14	59°	58.6°	95%	2.2°
15	216°	214.1°	90%	2.3°
<b>Mean</b>	-	-	<b>82%</b>	<b>3.4°</b>

which is inverted to find the arrival amplitudes and phases. Should this be the case, using singular value decomposition to invert the matrix as opposed to the inversion lemma [4] may eliminate this problem.

The error in the AOA estimate for those solutions which were correct is very high. Using more points may improve the accuracy. Tests with narrower clusters (10° as opposed to 50°) indicate that cluster width strongly affects the accuracy. It appears that temporal MUSIC does not average a cluster of arrivals as well as spatial MUSIC does in technique #1.

#### H. Technique #4—Temporal Music and One Cluster

Temporal MUSIC was also applied to the problem of finding the strongest arrival in a cluster of 13. In this case, the assumption that a LOS cluster exists is extended such that within the cluster, a single LOS arrival exists with considerably greater power than the others. This technique can therefore be used in conjunction with the previous three techniques to fine tune the AOA estimate within one cluster.

A total of 14 different clusters are used with 20 data sets per cluster. The LOS clusters of the cluster sets in Table IV are used with the exception of cluster set 13; cluster set 13 has the same LOS cluster as cluster set 4. Each cluster is again 50° ( $\pm 25^\circ$ ) wide, and the arrival closest to the angular center of the cluster is given a power 10 dB higher than that of the next most powerful arrival.

Two antennas separated by  $0.25\lambda$  (9 cm) are used. However, 25 virtual elements are used as opposed to the five in technique #3. With the points spread by  $0.1\lambda$ , 25 points are collected in 86 cm at 50 km/h.

Temporal MUSIC is asked to resolve for 13 signals, and the one with the highest amplitude is chosen as LOS. The results are shown in Table V. A “valid solution” is defined as for technique #3 above.

The results of Table V are considerably better than those in Table IV. Although the number of correct solutions is better, (82% in Table V as opposed to 52.8% in Table IV), the cause

of the incorrect solutions is the same. Errors in the phases prohibit the elimination of the ambiguity.

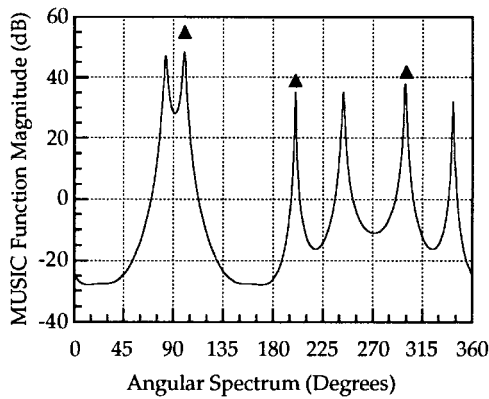
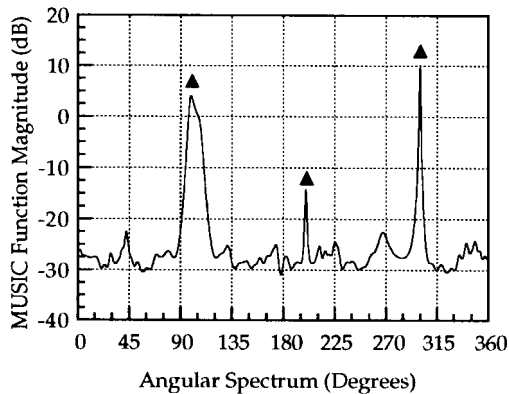
The error in the correct LOS solutions is much smaller compared to the results for finding the LOS cluster AOA in a three-cluster environment. This is most likely due to the fact that in the one-cluster environment, MUSIC is attempting to resolve for individual arrivals, one of which is of a significantly higher power, rather than trying to find an average AOA for a cluster.

#### IV. RESOLVING ALONG A CURVE

To this point, all simulated data have been generated for travel along a straight line. This has necessitated two antennas in order to generate a unique angular spectrum through 360°. If, however, a single antenna is sampled along a nonlinear trajectory, a 2-D array is formed. In order to eliminate the cosine ambiguity, the trajectory of the antenna must be sufficiently nonlinear. Part of this work was to determine how nonlinear the trajectory must be. Fig. 10 illustrates the spectrum generated by spatial MUSIC for an antenna travelling at 80 km/h along an arc of radius 20 m (a purely hypothetical situation—a slower velocity and lower sampling rate would result in the same number of points collected over the same angular distance). The sample points were collected over an angular distance of 2.6°. There are three signals present, and their AOA's are indicated by the black pointers. Although the three signals are accurately resolved, the cosine ambiguity is obvious by the spectral folds about 90° and 270°. Therefore, for the radius of the arc, the distance travelled is not sufficient.

Fig. 11 shows the spectrum for the same number of sample points, but spread over an arc of length 25°. In this case, there is sufficient curvature in the path travelled to remove the ambiguity. There is a price to pay for removal of the second antenna. In addition to knowledge of the distance between sample points (virtual elements) and the direction of travel, the trajectory of the path travelled is also required. Hence, there is a tradeoff between the cost of a second antenna and the complexity of determining the path trajectory.



Fig. 10. Resolving on a curve over  $2.6^\circ$ .Fig. 11. Resolving on a curve over  $25^\circ$ .

The quality of signal processing suffers when the antenna system travels along a curve. The steering vector can only be oriented for one direction of rotation. Hence, it is not possible to use both forward and backward smoothing. For spatial smoothing with subarrays, the steering vector must be of the same dimension as the subarrays and must therefore assume an average position along the curve travelled. This will affect both the magnitude of peaks in the MUSIC spectrum and the accuracy of the AOA estimates made.

Fig. 12 illustrates how far an antenna must travel along an arc in order to eliminate the cosine ambiguity. The simulated data is for one signal with AOA of  $246.7^\circ$ . The antenna travels at 20 km/h along an arc of radius 20 m. Data samples are obtained every half wavelength for a frequency of 840 MHz. In Fig. 12, the horizontal axis measures the length of the virtual array in degrees of arc as additional points are added every half wavelength. The individual measurement points are shown and the number of data points in the array varies from 3 to 40. The number of subarrays was always made to be an integer value of 0.75 of the array dimension.

The vertical axis measures the heights of the MUSIC spectrum peaks. The three curves correspond to the heights of the true peak, ambiguous peak, and spectrum floor. Plainly evident is that the cosine ambiguity disappears when the virtual array reaches a length of  $20^\circ$  of arc. For an arc of radius 90 m, an array length of  $10^\circ$  of arc was required. In terms of linear distance, the antenna must travel twice as far on the arc of radius 90 m than on the 20-m radius arc.

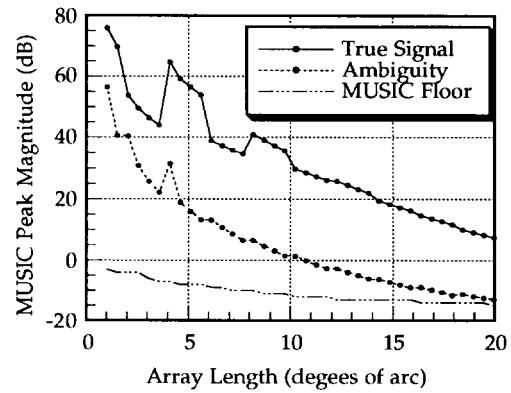


Fig. 12. Peak magnitude comparison.

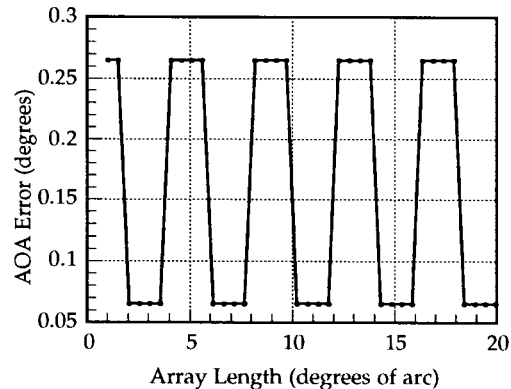


Fig. 13. Effect of steering vector on AOA accuracy.

Fig. 12 also shows one of the effects of the steering vector definition. As points are added to the virtual array, the number of subarrays will alternate between an even and odd number if the subarray dimension is held to 0.75 of the array dimension. One would anticipate that the subarray closest to the center of the array would be the best definition for the steering vector for the entire array. If there is an odd number of subarrays, a middle subarray exists whereas if the number of subarrays is even, none of the subarrays lie exactly in the middle of the array. The effect of this on peak height is visible in the curve corresponding to the true signal peak. Two distinct levels, defined by groups of four points, are recognized in the curve. The first two points correspond to arrays with an even number of subarrays, the next four to an odd number of subarrays and so on.

Perhaps more significant is the effect of the steering vector definition on the AOA accuracy. Fig. 13 shows the AOA error of the true peak as the virtual array is made longer by adding points spaced by a half wavelength. The horizontal axis is identical to that of Fig. 12. Two different AOA estimates, dependent on the steering vector definition, are seen. When there is an odd number of subarrays and the middle one is used to define the steering vector, the error in the AOA estimate is  $0.065^\circ$ . When the number of subarrays is even and one of the two most central subarrays is used to define the steering vector, the AOA error increases to  $0.265^\circ$ . Although the difference in accuracy in this case is very small, it does demonstrate that when spatial smoothing with subarrays is used, the steering

vector for the array should be as central as possible in the case of a curved array. When the trajectory of the antenna becomes more complex, it will be more difficult to define the steering vector for the case of smoothing with subarrays.

## V. CONCLUSION

MUSIC has demonstrated the ability to accurately resolve for the AOA of a number of coherent arrivals. When the arrivals are grouped in clusters, MUSIC is able to estimate the mean AOA of the clusters with some success.

Three techniques were used to determine which cluster in a three-cluster environment corresponds to LOS, and to estimate its AOA. Techniques #1 and #2, which use spatial MUSIC, clearly identified the LOS cluster and gave accurate AOA estimates in the order of  $5^\circ$ . These two techniques require a windowing algorithm to group solutions and identify the group which constitutes a majority. Technique #2 has the added complexity of grouping individual peaks in the spectrum into clusters, whereas technique #1 requires many AOA estimates to average over in order to obtain the accuracy reported.

Technique #3 uses temporal MUSIC. It is the most straight forward in its approach to identifying the LOS cluster. Although it suffers from poor accuracy, it uses far fewer points than techniques #1 and #2. Better performance would result if improvement in resolving the ambiguity was achieved.

MUSIC is able to resolve for the AOA of the single most powerful arrival in a cluster with an accuracy of better than  $4^\circ$ . A practical system would use one of techniques #1, #2, or #3 to first identify the LOS cluster and estimate its AOA. Spatial filtering to remove all other clusters would then be followed by technique #4, which gives a more accurate estimate of the LOS AOA.

An AOA accuracy of  $5.6^\circ$  (as achieved by technique #2) should be adequate to obtain a positional accuracy of 100 m or less in the microcellular radio environment. If two transmitters situated on a circle are  $90^\circ$  apart and the mobile receiver is located at the center of the circle, the minimum and maximum positional errors for AOA errors of  $5^\circ$  will be 11% and 14% of the circle radius respectively. Although a transmitter separation of  $90^\circ$  is perhaps the ideal case, using AOA estimates from multiple transmitters will give a positional accuracy better than 10% of the circle radius. Therefore, if the above-mentioned circles correspond to cells with radii in the order of 1 km, the desired positional accuracy will be obtained with AOA estimates made by techniques #1 and #2.

The accuracy of all the above techniques may be improved by the use of root-MUSIC in place of standard MUSIC [4]. There may also be a computational advantage in that root-MUSIC does not require scanning of the angular spectrum.

A vehicle location system incorporating MUSIC could use the existing mobile cellular telephone infrastructure. Additional requirements are some signal processing at the vehicle as well as an additional antenna. Should sufficient accuracy be obtained when sampling one antenna while traveling a nonlinear path, the existing mobile cellular telephone antenna system would be adequate.

## ACKNOWLEDGMENT

The authors wish to acknowledge the feedback of the reviewers which improved the quality of this paper.

## REFERENCES

- [1] S. Sakagami, S. Aoyama, K. Kuboi, S. Shirota, and A. Akeyama, "Vehicle position estimates by multibeam antennas in multipath environments," *IEEE Trans. Veh. Technol.*, vol. 41, no. 1, pp. 63–68, 1992.
- [2] G. Morrison, M. Fattouche, and D. Tholl, "Parametric modeling and spectral estimation of indoor radio propagation data," in *Proc. Wireless '92*, TRLabs, Calgary, Alberta, Canada, July 8–10, 1992.
- [3] Cellular System, "Dual-mode mobile station-base station compatibility standard," EIA/Interim standard 54-B, Electronic Industries Association, May 1990.
- [4] S. Haykin, *Adaptive Filter Theory*, 2nd ed. Englewood Cliffs, NJ: Prentice-Hall, 1991.
- [5] R. O. Schmidt, "Multiple emitter location and signal parameter estimation," *IEEE Trans. Antennas Propagat.*, vol. AP-34, no. 3, pp. 276–280, 1986.
- [6] F. Haber and M. Zoltowski, "Spatial spectrum estimation in a coherent signal environment using an array in motion," *IEEE Trans. Antennas Propagat.*, vol. AP-34, no. 3, pp. 301–310, 1986.
- [7] S. U. Pillai and B. Y. Kwon, "Forward/backward spatial smoothing techniques for coherent signal identification," *IEEE Trans. Acoust., Speech, Signal Processing*, vol. 37, no. 1, pp. 8–15, 1989.
- [8] P. A. Goud, "A spread spectrum radiolocation technique and its application to cellular radio," M.Sc. thesis, Univ. Calgary, Canada, Aug. 1991.
- [9] H. Hashemi, "Simulation of the urban radio propagation channel," *IEEE Trans. Veh. Technol.*, vol. VT-28, pp. 213–225, Aug. 1979.
- [10] G. L. Turin, F. D. Clapp, T. L. Johnston, S. B. Fine, and D. Lavry, "A statistical model of urban multipath propagation," *IEEE Trans. Veh. Technol.*, vol. VT-21, pp. 1–9, Feb. 1972.
- [11] H. Suzuki, "A statistical model for urban radio propagation," *IEEE Trans. Commun.*, vol. COM-25, pp. 673–680, July 1977.
- [12] Private communication with H. Hashemi, Sharif Univ. Technol., Tehran, Iran.

**Richard Klukas** received the B.Sc. and M.Sc. degrees in electrical engineering in 1989 and 1993, respectively, and the Ph.D. degree in geomatics engineering in 1998, all from the University of Calgary, Calgary, Alberta, Canada. The topic of his dissertation was a cellular telephone positioning system using superresolution and GPS time synchronization.

Before entering graduate school, he worked as a Test Engineer at Northern Telecom Canada in the Digital Switching Division. He is currently the Director of Research at Cell-Loc, Inc., Calgary, a company specializing in cellular telephone positioning.



**Michel Fattouche** received the B.Sc. degree in electrical engineering from Cairo University in 1979, the B.Sc. degree in applied mathematics from Ain Shams University in 1981, and the M.Sc. and Ph.D. degrees from the University of Toronto, Toronto, Canada, in 1982 and 1986, respectively.

He joined the Department of Electrical and Computer Engineering, University of Calgary, Calgary, Alberta, Canada, as an Assistant Professor in 1986, where he is currently a Professor. He is also an Adjunct Professor with the Calgary-based wireless division of TRLabs, a research consortium of telecommunication companies. He has five patents issued and four patents pending in the field of wireless communications. He cofounded Wi-LAN, Inc. in 1992, Cell-Loc, Inc., Calgary, in 1995, and Wireless, Inc. in 1997. From 1993 to 1997, he was VP of Research of Wi-LAN, Inc., where he is currently VP of Engineering. From 1996 to 1997, he was President of Cell-Loc, Inc., where he is currently Chief Technical Officer. He is on the Board of Directors for Wi-LAN, Inc., Cell-Loc, Inc., Wireless, Inc., and the University of Calgary Engineering Endowment Foundation.